Accurate pH sensing via hyperpolarized ^{129}Xe NMR

Patrick Berthault, Estelle Léonce, Jean-Pierre Dognon, Delphine Pitrat, Jean-Christophe Mulatier, Thierry Brotin

Accurate pH sensing via hyperpolarized ^{129}Xe NMR

Estelle Léonce,[a] Jean-Pierre Dognon,[a] Delphine Pitrat, [b] Jean-Christophe Mulatier,[b] Thierry Brotin,[b] and Patrick Berthault*[a]

Abstract: In the search for powerful non-invasive methods for pH measurement, NMR usually suffers from biases, especially for heterogeneous samples or tissues. In this Communication, using the signals of hyperpolarized ^{129}Xe encapsulated in a pair of water-soluble cryptophanes, we show that a differential pH measurement can be achieved, free from most of these biases, by monitoring the difference between their chemical shifts.

Measuring non-invasively and in a local way the *in vivo* extracellular pH is of importance for the diagnosis of insidious pathologies such as cancers.[1] Different NMR approaches exist in that purpose, based either on endogenous or exogenous species and nuclei, but the crucial point is to overpass the sensitivity limitations of this modality. For one decade, the use of hyperpolarized agents, which nuclear polarization is transiently enhanced by several orders of magnitude, has been proposed.[2] DNP-hyperpolarized ^{13}C bicarbonate enables the extraction of tissue pH through measurement of the intensity ratio between ^{13}C NMR signals of bicarbonate and CO_2.[3] Also, Korenchan *et al.* monitored the ^{13}C chemical shift variation of DNP-hyperpolarized [2-^{13}C,D10]diethylmalonic acid (DEMA) with pH.[4] NMR pH sensing with SABRE[5]-hyperpolarized ^{15}N imidazole used the ^{15}N chemical shift difference between the protonated and deprotonated forms of the molecule.[6] Laser-polarized xenon reversibly encapsulated in cage-molecules bearing ionizable groups was shown to exhibit a pH-dependent chemical shift.[7] In the same domain, more sophisticated probes were proposed, however at the price of more complex molecular constructs.[8] In this non-exhaustive list, each method possesses its own advantage and inconvenience, and their applicability in the *in vivo* domain is not always straightforward.

Here we present an approach, which is simple, fast to implement and free from most of the biases that can be encountered *in vivo*. The idea is to perform a differential measurement by using a pair of pH-sensitive ^{129}Xe NMR-based sensors, instead of only one as in ref. [7]. The difference between the chemical shifts of xenon encapsulated in both molecular sensors will give access to pH. The method is rendered very pH-sensitive *via* the choice of two xenon host molecules in which the frequencies of the noble gas signals vary in opposite manner with the H^+ concentration. DFT calculations taking into account relativistic effects explain this behavior and give clues for the design of new ^{129}Xe NMR-based pH sensors.

For this proof-of-concept, the two cryptophanes described in Scheme 1 have been used. The synthesis of compound **1** is known.[9] The synthetic route used to prepare cryptophane **2** is described in the Supporting Information section (see Figure S1). Briefly, compound **2** is obtained starting from a functionalized cyclotribenzylene derivative (CTB) decorated with three benzyl groups.[10] Scandium triflate ($Sc(OTf)_3$) used in catalytic amount allows us to promote the cyclisation of the second CTB unit of the cryptophane precursor. The reaction gives rise to a dissymmetrical cryptophane of C_3-symmetry bearing both phenol and benzyl functions located on each side of the cryptophane.[10,11] Herein, $Sc(OTf)_3$ has been preferred to other acids because this approach facilitates purification of the cryptophane derivatives especially when they are obtained in low yields. Then, three carboxylic acid groups protected by benzyl functions are introduced in a single step on the cryptophane skeleton. Finally, the removal of the benzyl groups by hydrogenation on Pd/C provides the desired compound **2**. Compound **2** has been fully characterized by ^{1}H and ^{13}C NMR spectroscopy and HRMS (see Figures S2 - S4 of the Supp. Info.).

Scheme 1. Structure of the cryptophanes used in this study.

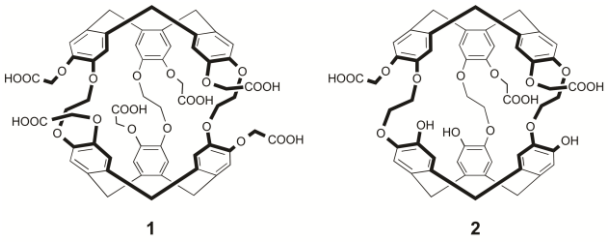

1 2

The combined use of these two xenon hosts has many advantages. They are both water-soluble in the 10^{-4} M range whatever the pH. They have comparable structures, based on a *anti* cryptophane-222 core. They bear the same functional groups (carboxylate groups), meaning that they will have nearly the same bio-distribution and behavior with respect to xenon, both for the thermodynamics and kinetics points of view.

According to ref. [7], at basic pH and 293K, xenon in cryptophane **1** resonates at 64.55 ± 0.10 ppm (using as reference the signal of xenon free in water calibrated at δ=196 ppm). The maximal xenon chemical shift variation with pH has been derived from a fit against the theoretical equation: δ_{acid}-δ_{base} = $\Delta\delta_1$ = 3.55 ± 0.17 ppm. The abscissa of the inflexion point of the sigmoid appears at pH_1 = 4.55 ± 0.05.

The interaction of xenon with cryptophane **2** had until now never been studied. Figure 1 displays the chemical shift of the noble gas encapsulated in **2** at 293 K for different pH values. At

[a] E. Léonce, Dr. Jean-Pierre Dognon, Dr. P. Berthault
NIMBE, CEA, CNRS
Université Paris Saclay, CEA Saclay
91191 Gif-sur-Yvette, France
E-mail: patrick berthault@cea.fr
[b] Dr. T.Brotin, D. Pitrat, J.-C. Mulatier
Laboratoire de Chimie de L'ENS LYON (UMR 5182)
Ecole Normale Supérieure de Lyon
46, Allée d'Italie
69364 Lyon Cedex 07, France

basic pH and 293K, xenon in cryptophane **2** resonates at 70.83 ± 0.10 ppm. Between pH 2 and pH 10 a sigmoidal fit against the suitable function (see Supp. Info.) enables location of the inflexion point at pH_2 = 3.03 ± 0.05. The maximal xenon chemical shift variation with pH is $\Delta\delta_2$ = -2.19 ± 0.14 ppm.

It is worth noting that although the fits of the data points by the theoretical curve are good for both cryptophanes, a large uncertainty may appear in the method, especially for cryptophane **2** that exhibits a more reduced chemical shift variation for encapsulated xenon.

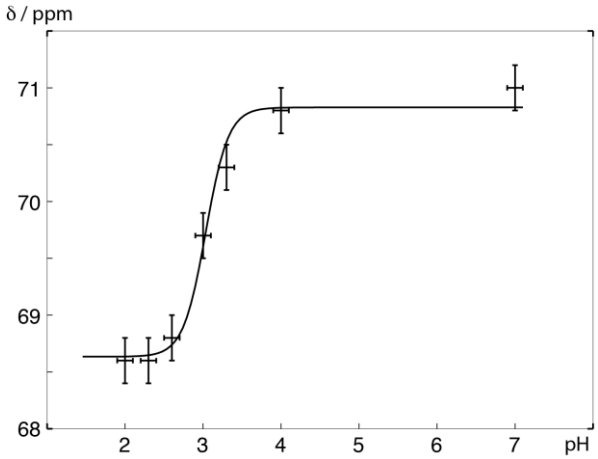

Figure 1. Plot of the chemical shift of xenon caged in **2** as a function of pH and fit by the function *f2*, see Supporting Information.

Indeed, the caged xenon chemical shifts are referenced to the signal of xenon free in solution, arbitrarily calibrated. But independent ^{129}Xe NMR measurements have shown that this value can fluctuate depending on the nature of the bulk solvent. For instance, a modification of the ionic strength or the simple nature of the buffer (see Figure S5 of the Supp. Info.) can have a strong impact on the ^{129}Xe chemical shift. Thus, the measured caged xenon chemical shift values taken alone are only indicative and the deviation of some points can be due to the presence of other ions in solution.

Nevertheless, such a difference in behavior for the two cryptophanes led us to use a mixture of them as a differential probe of pH. Instead of measuring the chemical shift splitting between free and encapsulated xenon, the interesting parameter is now the difference δ(Xe**@2**) - δ(Xe**@1**) = $\Delta\delta_{12}$. Figure 2 displays the evolution of $\Delta\delta_{12}$ as a function of the pH of the solution. Here, near the pK_a of the carboxylic groups, the variation in the chemical shift difference is steep, providing a very high precision in the measurement of the pH in this region.

Figure 2. Plot of the chemical shift difference δ(Xe**@2**) - δ(Xe**@1**) with pH and

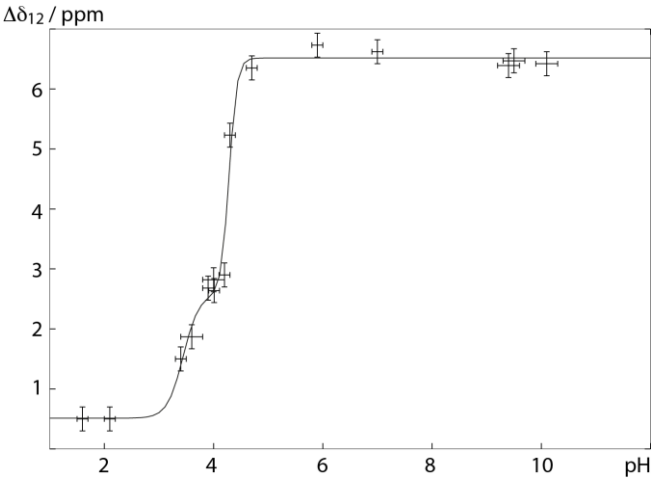

fit by he function *f3*, see Supporting Information.

The best fit with the theoretical function expressing the difference between the two sigmoids is superimposed on Fig. 2. The extracted parameters are the following: two inflexion points at pH_1 = 4.28 ± 0.02 and pH_2 = 3.44 ± 0.08, the maximal chemical shift difference $\Delta\delta_{12}^{max}$ = 6.51 ± 0.12 ppm, the minimal chemical shift difference $\Delta\delta_{12}^{min}$ = 0.51 ± 0.08 ppm.

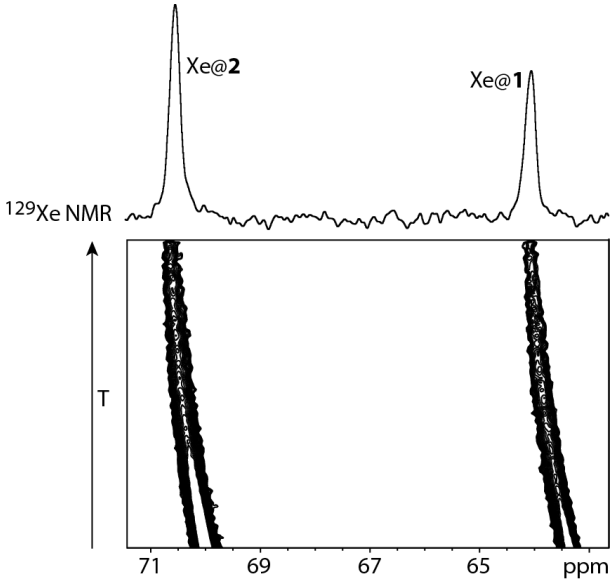

Figure 3. Evolution of the Xe@cage NMR signals (contour plot view) as a function of temperature (from 15° to 25°C) for a mixture of cryptophanes **1** and **2** at pH 8. It is worth noting that the chemical shift difference between them remains constant.

The robustness of the method to temperature and ionic strength variations has been assessed. Figure 3 represents the behavior of the caged xenon signal as a function of temperature. From this plot, it is clear that whereas the frequencies of the

signals of xenon caged in **1** and **2** vary with temperature, their difference is constant. A close examination of the successive spectra indicates that $\Delta\delta_{12}$ decreases by only 0.01 ppm for a temperature change of 10 degrees.

The effect of ionic strength on the xenon chemical shifts has also been studied. While an effect can be observed on the chemical shift of free xenon, no or non-significant variation of the $\Delta\delta_{12}$ value is observed upon saturation with a NaCl solution.

Although solubility could be a concern for the quantitative analysis of the signal intensities, it does not affect the pH measurement, as the splitting between the caged xenon signal is fully independent on concentration.

We have tested our capability to perform ^{129}Xe localized spectroscopy and to measure local pH in several regions by this method. In this purpose, a dedicated setup has been installed, using an NMR tube with two compartments filled with the mixture of cryptophanes at two different pH. Figure 4 displays the result of a spectroscopic imaging experiment, for which each pixel contains the high field part of the corresponding ^{129}Xe NMR spectrum.

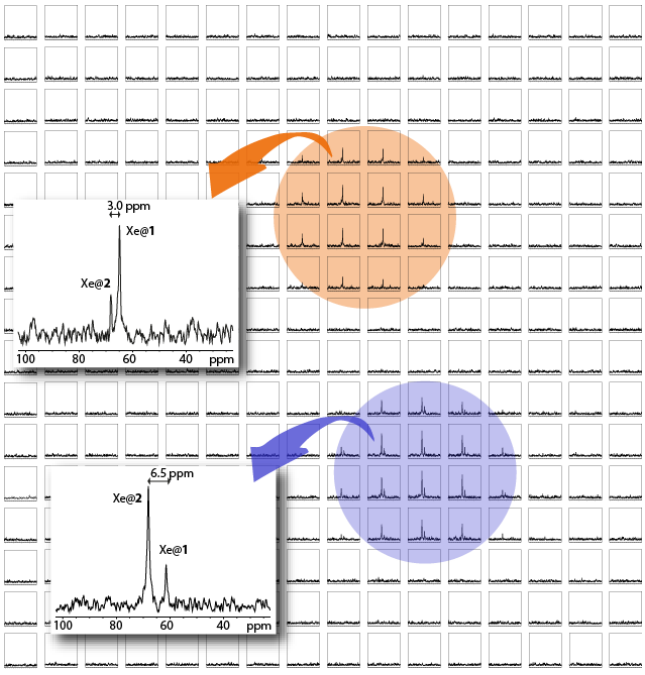

Figure 4. ^{129}Xe magnetic resonance spectroscopic imaging for pH sensing. Two tubes of inner diameter 2.3 mm contain a mixture of cryptophanes **1** and **2** at pH 4 (orange) and pH 9 (purple). The concentrations range between 150 and 250 µM. Other details: see text and Supporting Information.

As exemplified here, extracting the local pH from the ^{129}Xe chemical shift splitting is relatively easy. A value of 3.0 ppm on the ^{129}Xe spectra arising from the first compartment (orange region on Fig. 4) indicates that the pH of the solution is 4, while for the other compartment a chemical shift difference of 6.5 ppm corresponds to a pH value of 9 (purple region).

The fact that the evolution of the Xe**@2** chemical shift with pH is opposite to that of the Xe**@1** chemical shift is notable. Density functional theory (DFT) calculations have been carried out to provide explanation at the molecular scale for the origin of this chemical shift behavior (see Supp. Info. for details). The electric field gradient (EFG) on the site of the xenon nucleus is a well-suited tool to explore the role of molecular structure, electric charge distribution within the molecule and intermolecular interactions on the variation of the ^{129}Xe NMR-parameters upon substitution.

The asymmetry parameter η strongly depends on the local site symmetry. The ionization of the carboxylate groups in Xe**@1** induces little change in V_{zz} (the main component of the EFG tensor) with an increase of the symmetry (as reflected by η, see Table S1 and Figure S10 of the Supp. Info.) while in Xe**@2**, the asymmetry increases with a large change in V_{zz} (opposite sign). These evolutions come from a modification of the interactions between the xenon atom and the cage. The main interaction stabilizing the complex is the van der Waals (dispersion) interaction between xenon and the cryptophane phenyl ring, as shown by an energy decomposition analysis (see Figure S8 in Supp. Info.). A significant difference is also obtained in the Pauli repulsion and electrostatic interaction resulting in different steric interactions between Xe**@1** and Xe**@2**. These elements are at the origin of the change in the geometry from Xe**@1** to Xe**@2** upon ionization of the carboxylate groups with consequence a significant change (and opposite) of the chemical shift as measured and computed.

This approach using two cryptophanes properly chosen possesses many qualities. It is simple, robust against temperature, ionic strength and solvent effects as previously shown, and sensitive. As the introduction of xenon is fully decorrelated from that of the cryptophane mixture, it means that i) the quantity of xenon host introduced can be very low, reducing the risks of toxicity, ii) the question of the xenon relaxation time is not as crucial as for other hyperpolarized species. Indeed, here there is no limitation to one-shot experiments: the cryptophane mixture can be delivered once, then many NMR experiments can be performed with different xenon batches (a protocol all the more easy as the production of hyperpolarized xenon via optical pumping is quick). A fast xenon relaxation (such as in blood) will obviously lower the sensitivity of the approach, but to an extent, which is acceptable. Also the continuous in-out xenon exchange will enhance the sensitivity of the method by several orders of magnitude and will pave the route to experiments of the HyperCEST-type.[12] Figure S11 of the Supporting Information shows that alternatively to direct detection *via* fast repetition of soft pulses as in Figures 3 and 4, low quantities of cryptophane mixture can be detected in one scan through ^{129}Xe Ultrafast Z-spectroscopy.[13] Playing with the saturation strength and with the respective amplitudes of the saturation and acquisition gradients enables a net separation between the two dips corresponding to the caged xenon resonance frequencies.

Obviously, the pH range that can be probed with the current cryptophane pair lies in the region 3.5 - 5.5, owing to the ionizable groups grafted on them. It cannot be used for biological or biomedical applications. But this concept can be extended to other cryptophane pairs. For instance, cryptophane derivatives

decorated with citric acid or diethylmalonic acid functions are promising since some acidic functions show pk_a values close to the physiological pH. This work is underway in our laboratories.

It is noteworthy that these cryptophanes may present different solubilities in tissues or different bio-distribution in tissues thus impeding the simultaneous detection of two caged xenon signals at the same location. This problem could be overcome by linking cryptophanes to each other. Bis-cryptophanes, whose synthesis has already been mastered by Brotin *et al.*,[14] could be a solution to have in one molecule the expected differential pH probe.

In any case, DFT calculations explicitly including relativistic effects have enabled us to understand the physical effects responsible of the opposite caged xenon chemical shift variation with pH for two cryptophanes with quasi-similar structures, and to propose other structures.

This integrated approach, helped by dedicated computational methods, thus paves the route to powerful pH sensors. The differential character of the measure leads to a pH sensor exempt of most of the errors usually encountered[15] and should constitute a precious tool for *in vivo* pH mapping. Indeed, unlike other NMR approaches, it is robust against magnetic susceptibility variations. Longitudinal monitoring of pH will be simply performed by introduction of fresh hyperpolarized xenon (via inhalation or injection in intralipid emulsions) as long as desired, well after the molecular cages have been delivered to the target organ. For these cages a micromolar concentration will be sufficient to run the experiment.

Experimental Section

Synthesis of the pH sensors. Cryptophane **1** possesses a D_3-symmetry and has already been prepared in both its racemic and enantiopure forms. The full synthesis of compound **1** and its enantiopure derivatives has been reported in the literature.[9,16-17] The detailed synthesis of cryptophane **2** (C_3-symmetry) and its binding properties with cationic species will be reported separately. Compound **2** was successfully isolated in small quantities and properly purified for the ^{129}Xe NMR experiments.

NMR experiments. Except for characterizing compound **2**, for which the NMR experiments were performed at 7 Tesla all the experiments were performed on a 11.7 T Bruker Avance II narrow bore spectrometer, using either a broadband 5 mm inverse probehead or a micro-5 probehead and a dual ^{129}Xe/^{1}H insert of 8 mm (for Figure 4).

^{129}Xe NMR experiment at variable temperature. The spectra recorded at different temperatures were obtained by freezing laser-polarized xenon inside the NMR tube, on top of the solution containing both cryptophanes (which is at the temperature of interest), and then vigorously shaking the tube previously thermalized 10°C lower than the setpoint temperature of the probehead, quickly inserting it in the NMR magnet and immediately starting the acquisition.

^{129}Xe magnetic resonance spectroscopic Imaging. The experiment was constituted by 16 phase encoding gradient values in the x and y dimensions. Other details: see Supporting Information.

Acknowledgements

We thank our glassblower Bruno Coltrinari for the construction of the two-compartment NMR tube used for the spectroscopic imaging experiment.

Keywords: NMR • hyperpolarized xenon • pH mapping • cryptophane • quantum chemistry

[1] R. J. Gillies, N. Raghunand, M. L. Garcia-Martin, R. A. Gatenby, *IEEE Eng. Med. Biol. Mag.* **2004**, *23*, 57–64.

[2] C. Hundshammer, S. Düwel, F. Schilling, *Isr. J. Chem.* **2017**, *57*, 788–799.

[3] F. A. Gallagher, M. I. Kettunen, S. E. Day, D. E. Hu, J. H. Ardenkj\a er-Larsen, R. in `t Zandt, P. R. Jensen, M. Karlsson, K. Golman, M. H. Lerche, et al., *Nature* **2008**, *453*, 940–944.

[4] D. E. Korenchan, C. Taglang, C. von Morze, J. E. Blecha, J. W. Gordon, R. Sriram, P. E. Z. Larson, D. B. Vigneron, H. F. VanBrocklin, J. Kurhanewicz, et al., *Analyst* **2017**,*142*, 1429-1433.

[5] R. W. Adams, J. A. Aguilar, K. D. Atkinson, M. J. Cowley, P. P. Elliott, S. B. Duckett, G. G. R. Green, I. G. Khazal, J. López-Serrano, D. Williamson, *Science* **2009**, *323*, 1708–1711.

[6] R. V. Shchepin, D. A. Barskiy, A. M. Coffey, T. Theis, F. Shi, W. S. Warren, B. M. Goodson, E. Y. Chekmenev, *ACS Sens.* **2016**, *1*, 640–644.

[7] P. Berthault, H. Desvaux, T. Wendlinger, M. Gyejacquot, A. Stopin, T. Brotin, J.-P. Dutasta, Y. Boulard, *Chem. Eur. J.* **2010**, *16*, 12941–12946.

[8] B. A. Riggle, Y. Wang, I. J. Dmochowski, *J. Am. Chem. Soc.* **2015**, *137*, 5542–5548.

[9] G. Huber, T. Brotin, L. Dubois, H. Desvaux, J.-P. Dutasta, P. Berthault, *J. Am. Chem. Soc.* **2006**, *128*, 6239 - 6246.

[10] T. Brotin, V. Roy, J.-P. Dutasta, *J. Org. Chem.* **2005**, *70*, 6187 - 6195.

[11] O. taratula, P. A. Hill, Y. Bai, N. S. Khan, I. Dmochowski, *Org. Lett.* **2011**, *13,* 1414–1417.

[12] L. Schröder, T. J. Lowery, C. Hilty, D. E. Wemmer, A. Pines, *Science* **2006**, *314*, 446–449.

[13] C. Boutin, E. Léonce, T. Bro in, A. Jerschow, P. Berthault, *J. Phys. Chem. Lett.* **2013**, *4*, 4172–4176.

[14] M. Darzac, T. Brotin, D. Bouchu, J.-P. Dutasta, *Chem. Commun.* **2002**, 48–49.

[15] J. J. H. Ackerman, G. E. Soto, W. M. Spees, Z. Zhu, J. L. Evelhoch, *Magn. Reson. Med.* **1996**, *36*, 674–683.

[16] J. Canceill, L. Lacombe, A. Collet, *J. Chem. Soc. Chem. Commun.* **1987**, 219 –221.

[17] A. Bouchet, T. Brotin, M. Linares, D. Cavagnat, T. Buffeteau, *J. Org. Chem.* **2011**, *76*, 7816-7825.